AIAA SciTech Forum
8–12 January 2018, Kissimmee, Florida
2018 Wind Energy Symposium

10.2514/6.2018-2020

Load Alleviation on Wind Turbines using Camber Morphing Blade Tip

Etana Ferede * and Farhan Gandhi †
Rotorcraft, Adaptive, and Morphing Structures (RAMS) Lab
Department of Mechanical, Aerospace, and Nuclear Engineering
Rensselaer Polytechnic Institute, Troy, NY, 12180, USA

This paper investigates the load alleviation capability of a camber morphing blade tip on multi megawatt scale HAWTs. A span-wise variation of camber at the outer blade region is proposed that blends seamlessly to the non-morphing part of the rotor blade. The NREL 5MW reference turbine is used as baseline design, where the outer 30% of the blade is linearly cambered with the maximum camber realized at the blade tip. The results obtained during simulations, following the IEC standard, indicate that the camber morphing blade tip is able to mitigate vibrational loads, such that reduction in fatigue loads range between 8%-37% for most wind turbine components. Furthermore, the controller is also capable of reducing ultimate loads due to extreme turbulence in the order of 30%-60%. Finally, a large reduction in peak-to-peak response, in the order of 43%-90%, is achieved for several turbine components under wind gust or extreme direction change.

I. Introduction

The Cost Of Energy (COE) is a key metric in the wind energy industry to evaluate the success of generating electricity from wind compared to other energy sources. Therefore, both the scientific community and the industry are continuously searching for ways to reduce the COE in order to make it competitive with already established methods for generating electricity. The cost of energy is reduced by increasing the Annual Energy Production (AEP). AEP is increased by expanding the rotor swept area in order to maximize energy capture from wind. As a result, the trend in wind energy industry is towards larger wind turbines, especially for offshore wind farms. Unfortunately, scaling of the existing wind turbine components increases the COE since AEP is proportional to the square of rotor radius while the cost of wind turbine components is proportional to the cubic of rotor radius. An alternative approach is to look at load alleviation methods allowing for increased rotor radius (hence larger AEP), while mitigating loads which reduces the cost growth rate of wind turbine components.

The loads on wind turbine components can be reduced using active or passive control methods, applied over the whole blade span or distributed. Among the available load control methods, the Individual Pitch Control (IPC) is gaining more acceptance by the wind energy industry.[1] Another full span load control is the bend-twist coupled rotor blades[2] , where the structural properties of these blades is used to passively alleviate the loads on wind turbine components. However, these methods are limited in terms of bandwidth due to inertia, and non local blade response. Furthermore, fatigue concerns on pitch bearings limits the applicability of IPC for load alleviation. The distributed methods for load mitigation are attractive by providing higher bandwidth and control of local blade response, allowing further reduction in loads. Among distributed control methods, the use of flaps[3–6] and tabs[7–10] are extensively researched in the wind energy community. Unfortunately, wind turbine blades with flaps or tabs suffer from loss in aerodynamic performance and increased noise due to turbulent flow generation at the control surface edges.

In the present study, active Camber Morphing Blade Tips (CMBT) are used to mitigate the vibratory loads on multi megawatt Horizontal Axis Wind Turbines (HAWTs). With a linear variation in camber from

*Research scientist, Mechanical, Aerospace, and Nuclear Engineering, ferede@rpi.edu
†Professor, Mechanical, Aerospace, and Nuclear Engineering, AIAA Associate Fellow, fgandhi@rpi.edu

maximum at the blade tip to zero at the inboard end of the active section, the CMBT can offer increased aerodynamic efficiency and reduced noise, since the cambered blade section blends seamlessly with the non-morphing section of the blade and hence no turbulent flows are generated that adversely affects the rotor performance. Load alleviation capability of the current method is evaluated using international certification standard within FAST,[11] a state-of-the-art aero-servo-elastic simulation tool for wind turbine load analysis.

II. Concept

This paper investigates the load alleviation capability of Camber Morphing Blade Tip on multi megawatt scale HAWTs. A span-wise variation of camber at the outer blade region is proposed that blends seamlessly to the non-morphing part of the rotor blade, as shown in Figure 1. Looking at Figure 1, linear camber

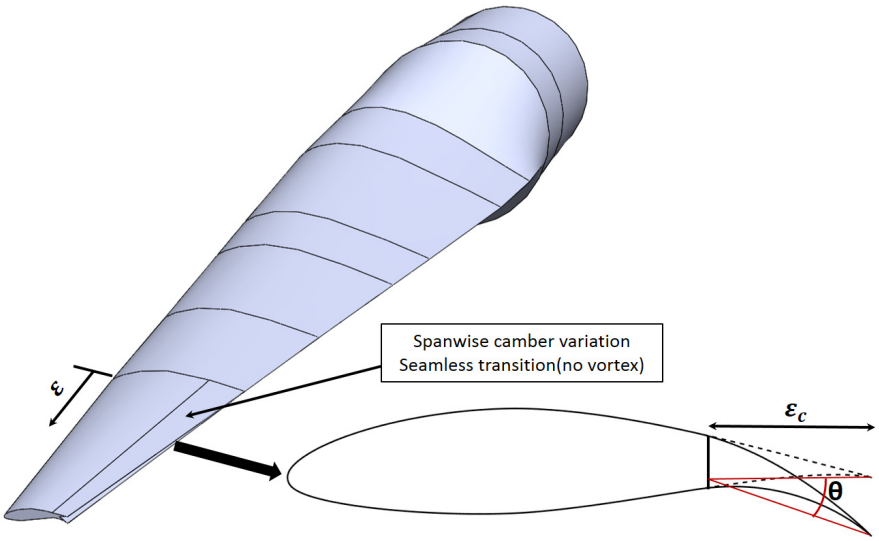

Figure 1. Concept of camber morphing blade tip.

variation along the blade span is implemented where the magnitude of morphing angle θ is given by:

$$\theta = \varepsilon\theta_{tip}, \tag{1}$$

linearly increasing towards the blade tip for $\varepsilon \in [0, 1]$, where θ_{tip} is the maximum morphing angle realized at the blade tip. Finally, chord-wise section of the airfoil with actively changing camber is denoted by ε_c in Figure 1.

III. Turbine

The NREL 5MW[12] reference turbine is used as the baseline turbine with the gross properties given in Table 1. The 5MW Machine is a pitch regulated turbine with a rotor diameter of 126m and a hub height of 90m. The current study does not include the underwater support structure in the modeling process. The outer 30% of the blade, consisting of the airfoil shape NACA 60-618, is linearly cambered with the maximum camber realized at the blade tip. On the airfoil section, the percentage of the chord designated for camber morphing is determined by performing a 2D analysis of an airfoil shape where the chord length of the trailing-edge camber section was varied parametrically. From the analysis, the NACA 60-618 airfoil with 30% of its trailing edge cambered is selected on the basis of sufficient change in lift (Δc_l) without significant increase in drag (high $\frac{\Delta c_l}{\Delta c_d}$) compared to the baseline airfoil. The change in airfoil shape is achieved by modifying the camber line. A quadratic function is added to the camber line, such that:

$$\Delta y_c = \begin{cases} 0 & \text{if } x < x_s \\ \dfrac{(x - x_s)^2}{C_f} \tan\theta, & \text{otherwise,} \end{cases} \tag{2}$$

Table 1. Gross properties for the 5MW reference turbine.[12]

Rating	5MW
Rotor orientation, Configuration	Upwind, 3 Blades
Control	Variable Speed, Pitch controlled
Rotor, Hub diameter	126 m, 3 m
Hub height	90 m
Cut-in,Rated,Cut-out wind speed	3 m/s, 11.4 m/s, 25 m/s
Cut-in,Rated rotor speed	6.9 rpm, 12.1 rpm

where Δy_c is a change in airfoil camber, x is the non-dimensional coordinate along the chord, x_s is the non-dimensional starting position for the morphing section of the airfoil, C_f is the length of the morphing section, and θ is the morphing angle.

The open source code FAST[11] is used for load analysis with the necessary modifications to the code in order to incorporate the effect of morphing blade tip during simulation. Particularly, the effect of cambered airfoils on the 2D aerodynamic characteristics is passed to FAST by including an additional input to the software. This external input allows for the aerodynamic module of FAST to interpolate, during simulation, the sectional aerodynamic properties using different 2D polar data for the same airfoil section and the morphing angle along the blade span. The 2D aerodynamic characteristics of the cambered airfoil are obtained for different morphing angle θ_{tip} using RFOIL,[13] evaluated for Reynolds number of nine million and over a range of angle of attack (see figure 2). FAST is developed and verified by NREL to serve as an

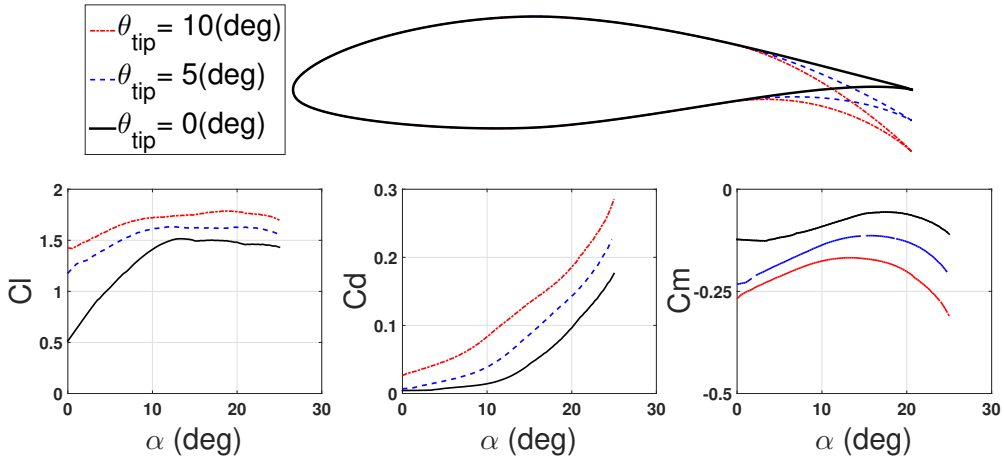

Figure 2. 2D aerodynamic characteristics of NACA60-618 airfoil for different morphing angle θ_{tip} and 30% of the chord cambered, evaluated at Reynolds number of 9×10^6 and for a range of angle of attack.

aero-hydro-servo-elastic tool for load analysis of horizontal-axis wind turbines. It is a time domain analysis tool making it suitable, among others, for fatigue load calculations. The latest version of FAST(FAST v8) is used in the present analysis. A combination of modal and multi-body dynamics is employed in FAST to model the structural dynamics of the wind turbine. Three mode shapes are used to model the blades: the first and second flap-wise mode shapes and first edge wise mode shape. The torsional degree of freedom is not included in modeling the structural dynamics of the blade. However, the torsional stiffness the NREL 5MW blade is sufficiently large such that the torsional degrees of freedom does not significantly contribute to the aeroelastic response of the blade. Aerodyn[14] is the aerodynamic module in FAST that calculates the aerodynamic loads on the blade that reads in stochastic wind data from Turbsim[15] or deterministic wind data from IECWind.[16] Two wake models: Blade Element Momentum(BEM) theory and Generalized Dynamic Wake(GDW) theory, are implemented in Aerodyn. The BEM theory with tip-loss and hub-loss corrections is used for the current analysis due to computational instability of GDW theory at low wind

speeds. Finally, a quasi-steady analysis is carried out which excludes the effect of dynamic inflow and unsteady 2D aerodynamics from the present analysis.

IV. Control layout

The control system layout used for present analysis is presented in Figure 3. The pitch and torque controller is an implementation of FAST turbine controller design.[12] In addition to the conventional controllers,

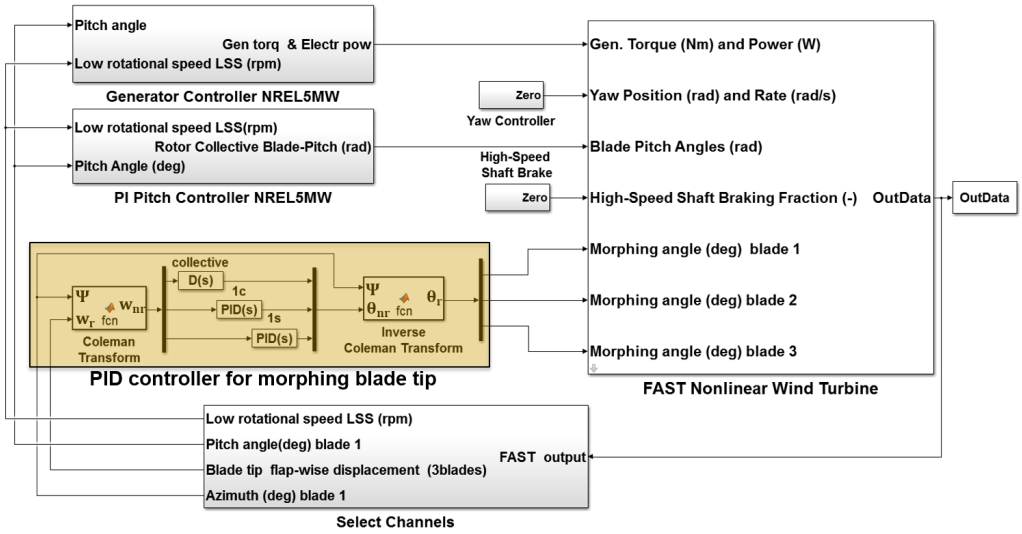

Figure 3. Turbine control layout.

a controller for the camber morphing blade tip is implemented. First, the controlled response, which is the out-of-plane (out-of-plane refers to the rotor plane) blade tip displacement w_{tip}, is transformed using the Coleman's transformation in collective (w^0_{tip}), yaw (w^s_{tip}), and pitch (w^c_{tip}) modes defined in the non-rotating frame,[17] such that:

$$\begin{Bmatrix} w^0_{tip} \\ w^c_{tip} \\ w^s_{tip} \end{Bmatrix} = \frac{2}{3} \begin{bmatrix} \frac{1}{2} & \frac{1}{2} & \frac{1}{2} \\ \cos\psi_1 & \cos\psi_2 & \cos\psi_3 \\ \sin\psi_1 & \sin\psi_2 & \sin\psi_3 \end{bmatrix} \begin{Bmatrix} w^1_{tip} \\ w^2_{tip} \\ w^3_{tip} \end{Bmatrix}, \tag{3}$$

where ψ_i and w^i_{tip} are respectively the azimuth angle and flap-wise tip displacement of blade i. Next, a PID controller for CMBT is formulated in the non-rotating frame, such that:

$$\theta^0_{tip} = K_d \frac{dw^0_{tip}}{dt}, \tag{4}$$

$$\theta^c_{tip} = K_p w^c_{tip} + K_i \int_0^t w^c_{tip} dt + K_d \frac{dw^c_{tip}}{dt}, \tag{5}$$

and

$$\theta^s_{tip} = K_p w^s_{tip} + K_i \int_0^t w^s_{tip} dt + K_d \frac{dw^t_{tip}}{dt}. \tag{6}$$

The proportional,integral and derivative gains are given respectively by K_p, K_i and k_d. The feedback control design applies only a derivative gain on the collective mode (w^0_{tip}) to avoid changing the mean of the generated power.

Finally, the morphing angle in the fixed-frame ($\theta^{fixed}_{tip} = \left\{\theta^0_{tip}, \theta^c_{tip}, \theta^s_{tip}\right\}$) is transformed back to the rotating frame using the inverse Coleman's transform, given by:

$$\begin{Bmatrix} \theta^1_{tip} \\ \theta^2_{tip} \\ \theta^1_{tip} \end{Bmatrix} = \begin{bmatrix} 1 & \cos\psi_1 & \sin\psi_1 \\ 1 & \cos\psi_2 & \sin\psi_2 \\ 1 & \cos\psi_3 & \sin\psi_3 \end{bmatrix} \begin{Bmatrix} \theta^0_{tip} \\ \theta^c_{tip} \\ \theta^s_{tip} \end{Bmatrix}, \tag{7}$$

where θ^i is the maximum morphing angle of blade i. The gains of the PID controller are tuned first by analyzing the frequency content of flap-wise blade root bending moment and tower-top yaw and pitch moment due to pure periodic or stochastic excitation, as shown in Figure 4. Referring to Figure 4, the blade

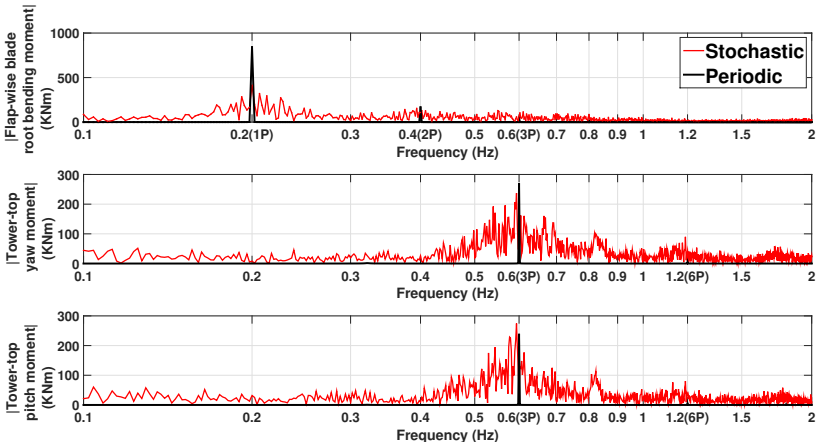

Figure 4. Frequency response of several turbine components due to periodic or stochastic excitation.

response for the periodic excitation (due to tower shadow and wind shear) is amplified at the multiples of the rotational speed, with the largest contributor being at $1P$. However, the frequency response of the blade, due to stochastic excitation (due to wind turbulence), is uniformly distributed across the frequency range of upto $1Hz$. In contrast, the tower response is excited mainly at $3P$, both for periodic and stochastic excitation of the turbine. The main contribution for fatigue loads, particularly for the blades, is analyzed in Figure 5. The Figure shows the normalized lifetime damage equivalent load (DEL) of the flap-wise blade root bending moment (RBM) as a function of the load frequency, due to excitation by turbulent wind including tower shadow and wind shear. It appears that about 90% of the damage is accumulated in the frequency range of upto $3P$. The gains are tuned, such that the $1P$, $2P$, and $3P$ of the out-of-plane blade tip displacement

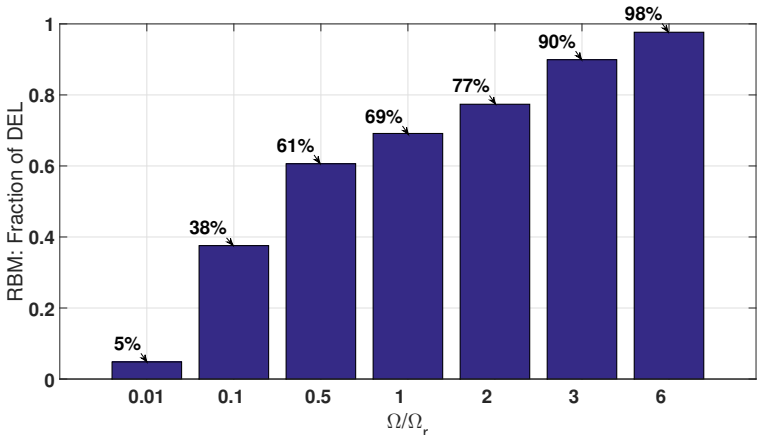

Figure 5. Normalized lifetime damage equivalent load (DEL) of the flap-wise blade root bending moment versus load frequency.

are significantly reduces (see Figure 6). Furthermore, Figure 6 shows that the control system is also able to reduce the $1P$, $2P$, and $3P$ components of the flap-wise blade root bending moment, and the $3P$ components of the tower-top pitch moment and rotor thrust. This should be sufficient to mitigate the fatigue loads and reduce the ultimate loads.

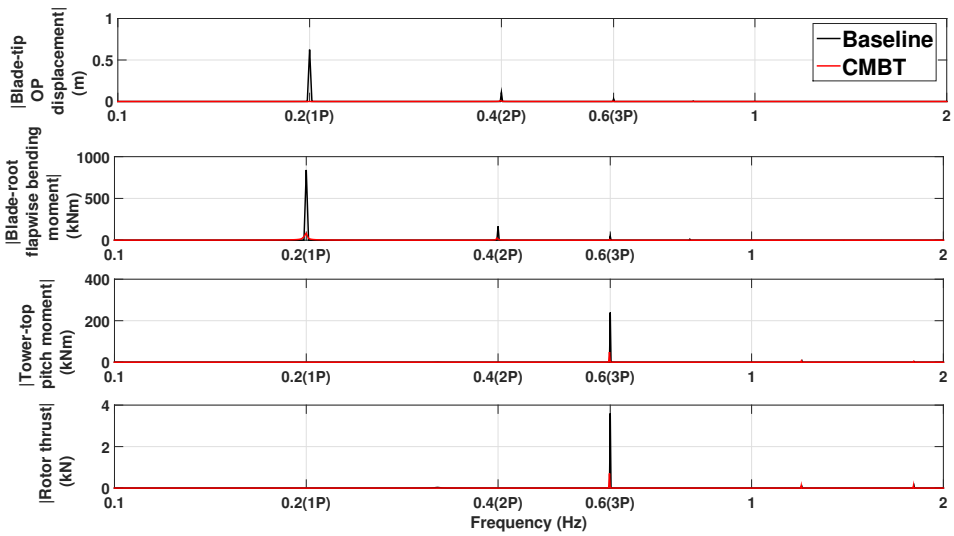

Figure 6. Frequency response for multiple turbine component due to periodic excitation, with and without controller (OP: out-of-plane).

V. Analysis cases

The performance of morphing blade tip is analyzed by considering several load cases from the International Electrotechnical Commision (IEC) 61400-1.[18] An overview of the considered loads cases from the IEC standard are listed in Table 2. These load cases cover power production with normal and extreme turbulence

Table 2. Considered load cases from IEC 61400-1.[18]

Design Load Case (DLC)	Wind type	Wind speed	Simulation time	Analysis
1.2 Power production	Normal turbulence Model	$U_{in} < U_h < U_{out}$	(4 times) 10min	Fatigue
1.3 Power production	Extreme turbulence model	$U_{in} < U_h < U_{out}$	10min	Ultimate
3.2 Start-up	Extreme operational gust	U_{rated}	4min	Ultimate
3.3 Start-up	Extreme direction change	U_{rated}	4min	Ultimate

U_h: hub-height wind speed, U_{in}: cut-in wind speed, U_{out}: cut-out wind speed, U_{rated}: rated wind speed @ hub-height

plus gust excitations during power production and during turbine start-up. Load cases for the IEC standard that cover parked condition, transportation, assembly, maintenance or repair are not considered since it is evident that the CMBT controller will not be used during these conditions. This also holds true for failure and emergency load cases from the IEC standard. Furthermore, the fatigue load case during turbine start-up(DLC 3.1) is omitted from the analysis since it is fair to assume that the load case pertaining to fatigue analysis during power production(DLC 1.2) is the design driver. Simulations where run for the baseline design and for the design with CMBT. In addition, the safety factors on the calculated loads are neglected, since they cancel out during a comparative study between controlled and uncontrolled case of the turbine.

For the first two load cases from Table 2, the turbulence wind fields are generated by TurbSim for a turbulence class of B and using the von karman turbulence model. For the remaining load cases, the deterministic wind fields are generated using EICWind. The wind shear profile is modeled using a power law with an exponent equal to 0.2. Finally, a Weibull distribution with a scale parameter 10.82 and shape parameter 2.15 is used for the hub height wind speed distribution, where the parameters are obtained from an offshore measurements in the Netherlands.[19]

The present study considers the loads throughout turbine in order to get a complete picture of the load reduction capability of the CMBT controller, see Figure 7.

VI. Reduction in fatigue loads

The first analysis considers fatigue loads. The design load case for power production(DLC 1.2) is considered since it contributes most to the fatigue damage. The fatigue damage of the turbine components

Figure 7. Monitored locations: blade root, nacelle, tower top and tower base (shown in dots).

is estimated using the NREL code MLife.[20] MLife gets as input a time history of the component loads, obtained by four times 10 minute simulations with different turbulence seeds in order to have a smooth estimation of the fatigue loads. Lifetime damage equivalent loads(DEL) are calculated using rain flow counting, Goodman relation, and Miner's cumulative damage rule.[21] The exponents in the S-N curve were set to 10 for the composite blades and 3 for the remaining turbine components. The overall performance of the camber

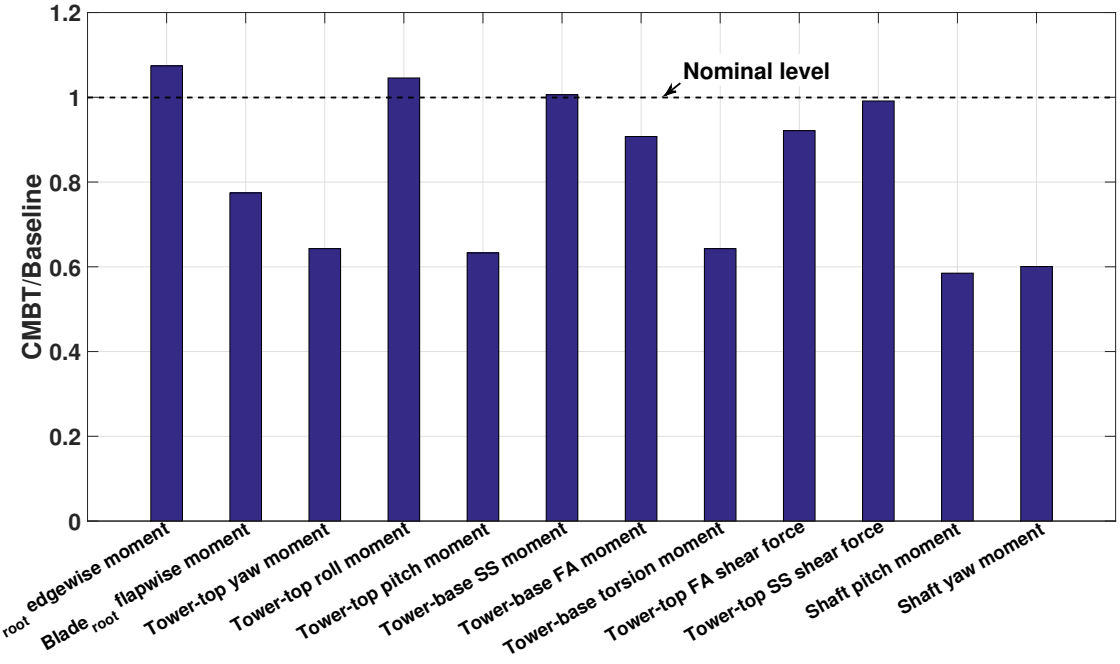

Figure 8. Fatigue damage ratio with and without CMBT controller(SS: side-side, FA: fore-aft).

morphing blade tip to reduce the fatigue loads on wind turbine components is shown in Figure 8, where the ratio between controlled and uncontrolled fatigue damage (lifetime damage equivalent loads integrated over the wind speeds) is displayed for several wind turbine components. It is shown that, for most turbine components, the fatigue damage is reduced or remains unaffected. A reduction of up to 24% is observed for the flap-wise blade root bending moment, while the reduction for the tower-top pitch and yaw moment are respectively, 37% and 36%. An in depth analysis of the major reduction potential of CMBT is carried out using Figures 9 to 11. Referring to Figure 9, the lifetime damage equivalent load for flap-wise root bending moment is reduced by about 22% at rated wind speed. The order of magnitude of the reduction is in good

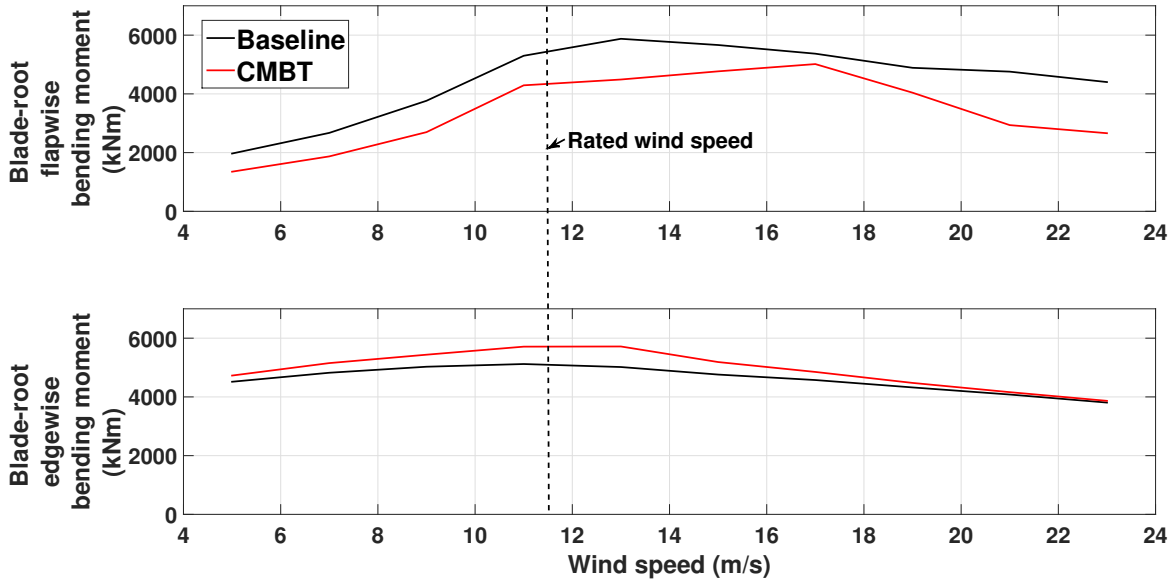

Figure 9. Damage equivalent load over turbines lifetime for load components at the blade-root, probability weighted.

agreement with[5, 22, 23] at rated wind speed. This modest reduction of the fatigue loads is the result of the current control design which is well suited in reducing the periodic components of the loading (due to tower shadow and wind shear). As shown in Figure 6, the controller is able to reduce the periodic loads, where it is sufficiently capable of reducing the $1P$, $2P$, and $3P$(for the blades) and $3P$(for the tower) components. Moreover, the highest reduction in damage equivalent load of 39% is observed at the cut-out wind speed. In contrast, the damage equivalent load for the edge-wise blade root moment is slightly higher for the controlled case across the wind speed range. This is the result of additional chord-wise loads generated due to camber actuation. A solution to this might be to use the morphing technology over the whole airfoil, such that a change in lift is achieved without resulting in unwanted change in drag. Furthermore, unlike the flap-wise blade root moment, which is aerodynamic driven, the edge-wise root bending moment is mainly driven by the gravitational load.[5] This is observed in Figure 9, where the fatigue damage for the edge-wise blade root bending moment does not vary significantly with wind speed. The results of Figure 6 indicate that reduction in out-of-plane blade tip displacement correlates well with reduction in flap-wise root bending moment but not with edge-wise root bending moment. A solution to this could be to use a control design, e.g. Linear Quadratic Regulator (LQR), that calculates the gain of the controller based on the full dynamic state of the blade.

Moreover, the camber morphing blade tip also has fatigue reduction capability of turbine components, other than the rotor. Figure 10 shows the damage equivalent load, over a range of wind speeds, respectively for the fore-aft (FA) shear force, pitch, and yaw moments at the tower-top. Below the rated wind speed, the CMBT controller reduced the DEL for the FA shear force but increases slightly for higher wind speeds between $13m/s$-$19m/s$. The net effect is that, using the CMBT controller, the fatigue damage for the FA shear force is sightly decreased by 8% (see Figure 8).

Furthermore, the controller reduced the damage equivalent load for the pitch and yaw moments, at the tower-top, respectively by 38% and 35% at rated wind speed. The steep reduction for these two components is a direct effect of the controller design. The gains of the controller are based on Coleman transformation of the out-of-plane blade tip displacement in yaw and pitch direction which strongly affect the aforementioned load components.

Finally, the CMBT controller is able to reduce the fatigue damage at the tower-base, as shown in Figure 11. A reduction of 35%, at rated speed, is observed for the torsional moment. There is in average no reduction in the side-side (SS) moment at the tower-base. The lack in reduction is to due to the fact that this load component is affected mainly by aerodynamic drag and gravitational load. It is already observed in Figure 9 that the controller is not able to mitigate vibration loads caused primarily by aerodynamic drag

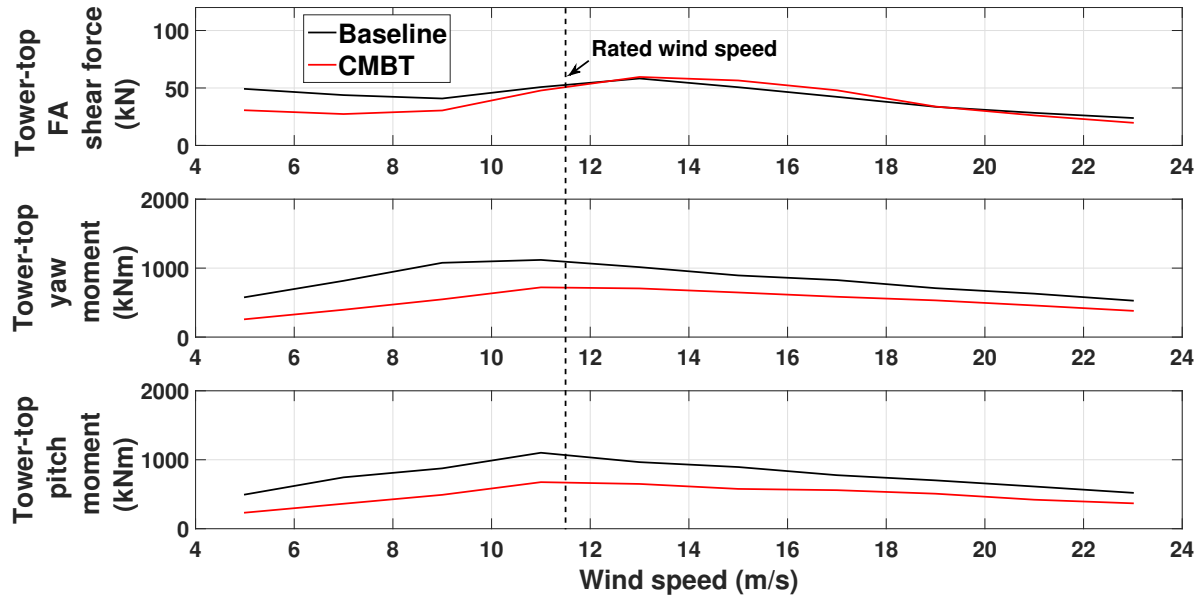

Figure 10. Damage equivalent load over turbines lifetime for load components at the tower-top, probability weighted.

and gravitational load. The controller is able to reduce the fore-aft (FA) moment at the tower-base for wind speeds below rated, with the highest reduction of 37% realized at the cut-in wind speed. There is a slight increase in the DEL load for wind speeds above the rated wind speeds. The FA moment is the sum of pitch moment at the tower-top and the FA shear force at the tower-top multiplied by the tower height. It is observed from Figure 10, that the highest reduction in DEL for the tower-top pitch moment and FA shear force occurs at low wind speeds (below rated), having a snowball effect on the DEL for the tower-base FA moment, where reduction in DEL is observed mostly for wind speeds below the rated wind speed. Overall, the cumulative fatigue damage for the FA moment is reduced by 10% with the CMBT controller, as shown in Figure 8.

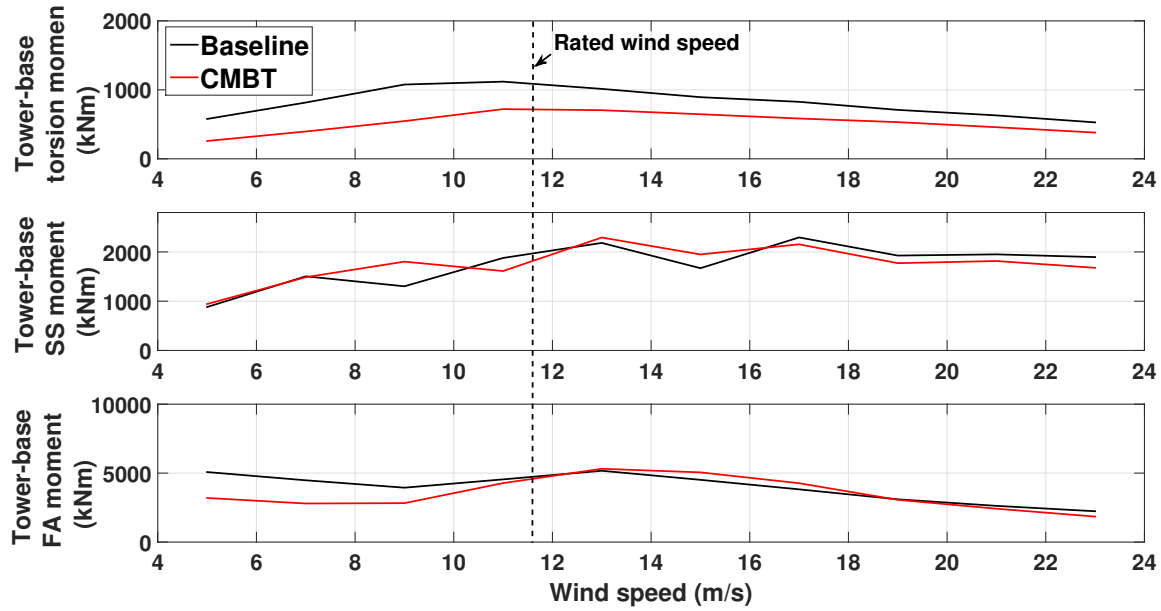

Figure 11. Damage equivalent load over turbines lifetime for load components at the tower-base, probability weighted.

From the controller side, the root mean square amplitude of the actuator deflection remains constant at 4° for all considered wind speeds (see Figure 12). This seems to indicate that the average actuator activity is constant across the wind speed spectrum. Looking at the frequency response of the actuator activity

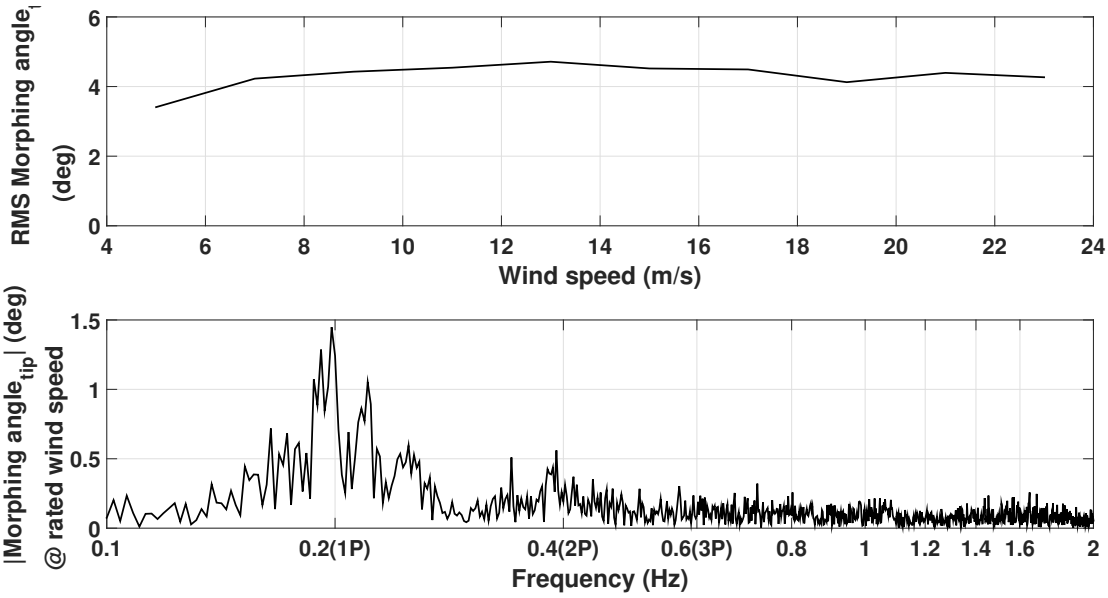

Figure 12. Morphing tip actuator activity vs wind speed(top) and frequency response of actuator at rated wind speed (bottom).

(bottom plot of Figure 12), at rated speed, the highest contribution to the actuator activity is around $1P$ and $2P$.

VII. Extreme loads mitigation

As the size of wind turbines increase, their design is increasingly driven by extreme loads than by fatigue loads. For example, tower clearance is becoming more crucial for up-wind turbines having long and flexible blades. This imposes a limit on the maximum flap-wise blade tip displacement making it a design driver for flexible blades. This requires to investigate the response of the turbine under extreme turbulence wind and several scenarios of wind gusts, given in the IEC standard.

A. Extreme turbulence

In addition to fatigue behavior, the effect of CMBT on the turbine response under extreme turbulence is examined. A ten minute simulation is carried out for hub height wind speed, between cut-in and cut-out wind speed, in accordance with design load case 1.3 from IEC standard. Figure 13 shows the load ratio between the controlled (CMBT) and uncontrolled (Baseline) case for various turbine components (sensors), evaluated at rated wind speed. At a glance, most of the sensors indicate load reduction when the controller is turned on. The flap-wise blade tip displacement is reduced by 27% with the CMBT actuator. A reduction of 14% is observed for the flap-wise blade root bending moment. There is a slight reduction in the tower-top SS shear force (5%) and tower base SS moment (3%). The roll moment at the tower-top also sees a slight reduction of 5%, while the blade root edge-wise bending moment sees an increase in extreme load by 32% when the CMBT controller is used. The increase in edge-wise moment is the result of additional chord-wise loads generated due to camber actuation. A solution to this could be to use the morphing technology over the whole airfoil, such that a change in lift is achieved without resulting in unwanted change in drag. A significant reduction is observed in the pitch moment, both for the tower-top and shaft, where a 48%-50% reduction is observed. Furthermore, the yaw/torsional moment at the tower-top, tower-base, and shaft see a decrease between 44% to 50% when the controller is turned on.

A further assessment of the load reduction capability of CMBT under extreme turbulence is presented in Figures 14 and 15. Figure 14 shows peak to peak response of the out-of-plane blade tip displacement (top)

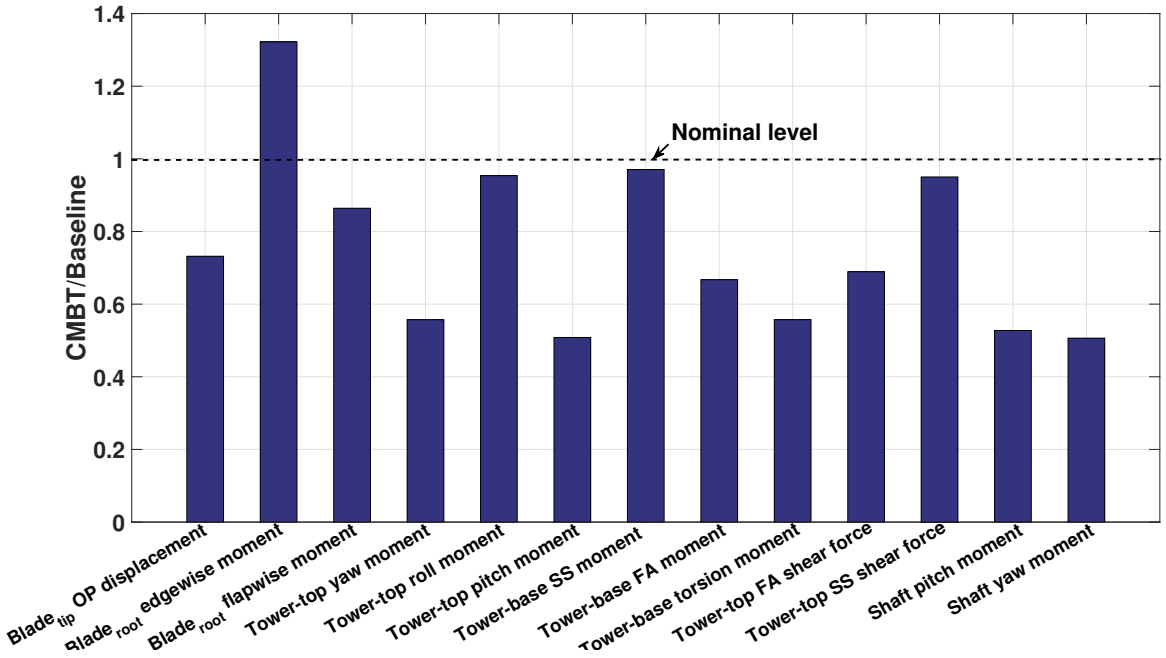

Figure 13. Peak-to-peak load ratio with and without CMBT controller due to extreme turbulence during power production, at rated wind speed (OP: out-of-plane, SS: side-side, FA: fore-aft).

and rotor thrust (bottom) as a function of the hub height wind speed. The controller is able to reduce the maximum out-of-plane blade tip displacement across the wind speed rage, with a largest reduction of 31% realized at the cut-out wind speed. Furthermore, it is observed that the reduction in blade tip displacement increases for increasing wind speed. There is modest reduction in the minimum blade tip displacement, with negligible reduction observed for low wind speeds. The controller is also able to reduce the yaw moment at the tower-top, across the wind speed range. A maximum reduction of 61% is realized at $15m/s$. The yaw

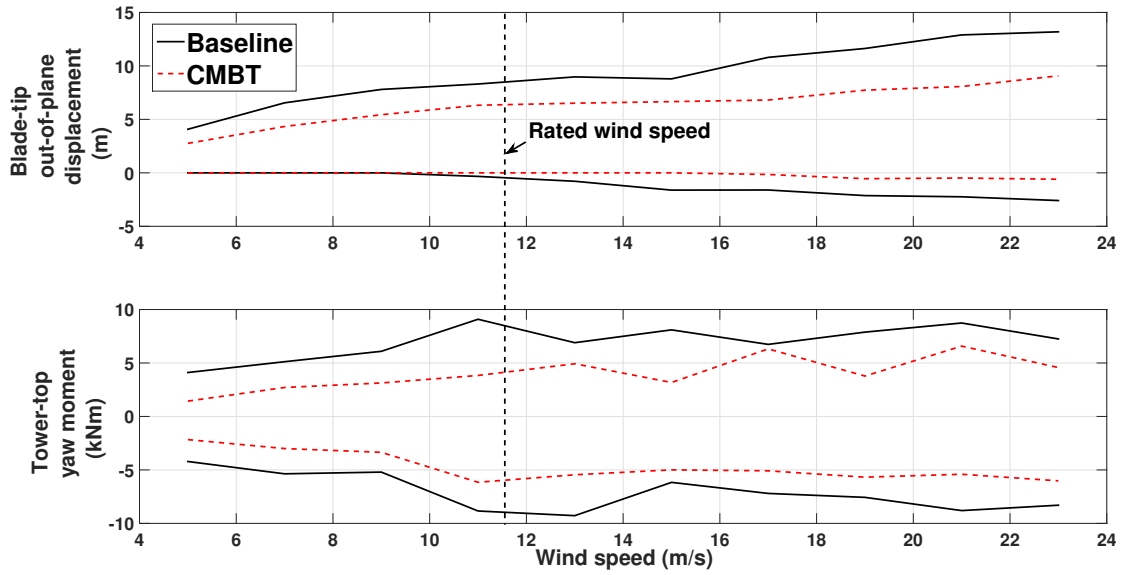

Figure 14. Extreme load vs wind speed due to extreme turbulence during power production.

moment at the tower-top is caused by asymmetric loading of the rotor disk, meaning that one side of the

rotor disk is more loaded than the other side, which is similar to the effect of wind shear. It is shown in Figure 6 that the controller is able to effectively mitigate load imbalance across the rotor disk.

The pitch moment at the tower-top and the FA moment at the tower-base see a load reduction when the CMBT controller is used. This is presented in Figure 15, where the first plot shows the pitch moment at the tower-top and the second plot depicts the FA moment at the tower-base across the wind speed range. Again, the ability of the controller to reduce load imbalance across the rotor disk is observed in Figure 15,

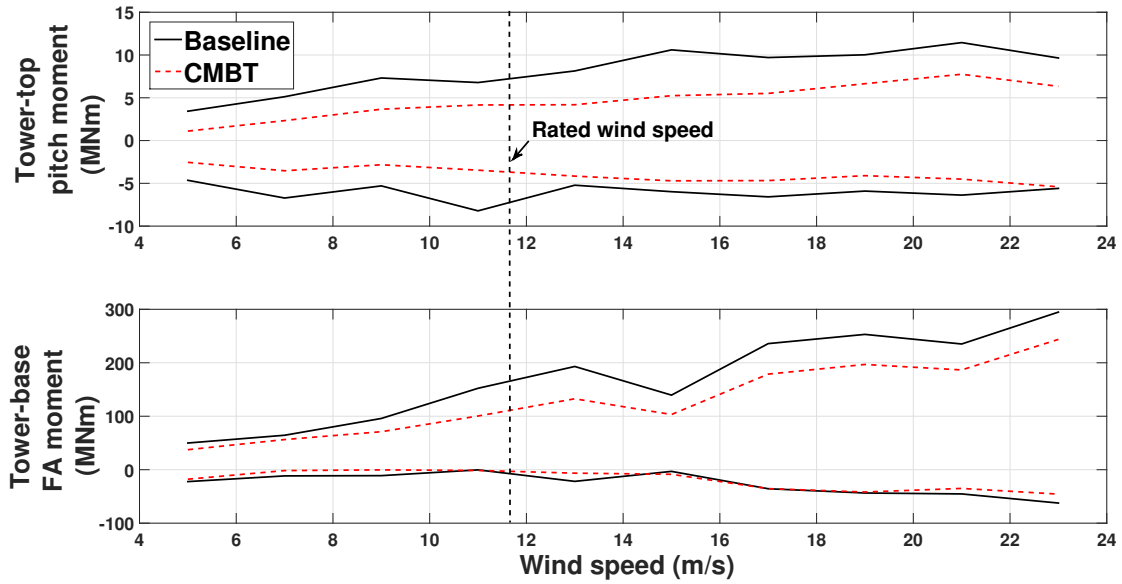

Figure 15. Extreme load vs wind speed due to extreme turbulence during power production.

where the pitch moment at the tower-top (caused mainly by wind shear and tower shadow) is reduced across the wind speed range, with a maximum reduction of 51% realized at $15m/s$. Furthermore, the peak load of the FA moment at the tower-base also sees decrease with the CMBT controller, across wind speed range. The reduction is mainly for the maximum peak loads. There is almost no reduction in the minimum FA moment. However, the peak-to-peak FA moment is reduced across the wind speed range, with the maximum reduction of 33% realized at hub-height wind speed of $13m/s$.

B. Extreme gust and change of direction

The last pertinent load cases from the IEC standard are: extreme gust (DLC 3.2), extreme direction change (DLC 3.3), and the combination of the two (DLC 1.4). A four minutes simulations are performed at rated wind speed. For all the load cases, the gust excitation starts two minutes into the simulation and lasts for ten seconds. Figures 16 and 17 show a load time history for various turbine components due to extreme operational gust and extreme direction change, respectively. At a first glance, it is observed that the controller is able to reduce all the peak loads for all turbine components and load cases. In the case of extreme gust (Figure 16), the reduction in peak loads, after removing the mean value, is: 76% for the out-of-plane blade tip displacement, 61% for flap-wise root bending moment, 46% for the rotor thrust, and 43% for the fore-aft moment at the tower-base. The controller is able to effectively mitigate the turbine response at the onset of the gust excitation. Furthermore, Figure 16 shows that the controller is able to reduce peak-to-peak load variation for all the turbine components shown in the figure. The CMBT controller performs equally well in reducing the peak loads due to extreme direction change (DLC 3.3), as shown in Figure 17. The peak-to-peak response of the load components, after *extreme change of direction*, increases for the uncontrolled case. This is effectively reduced by the controller, such that a reduction over 90% is achieved in peak-to-peak response of the out-of-plane blade tip displacement and over 71% reduction in peak-to-peak response for the flap-wise blade root bending moment. Furthermore, the rotor thrust and fore-aft (FA) moment at the tower-base see reduction, both in the mean and peak-to-peak value, with the CMBT controller turned on. The reduction

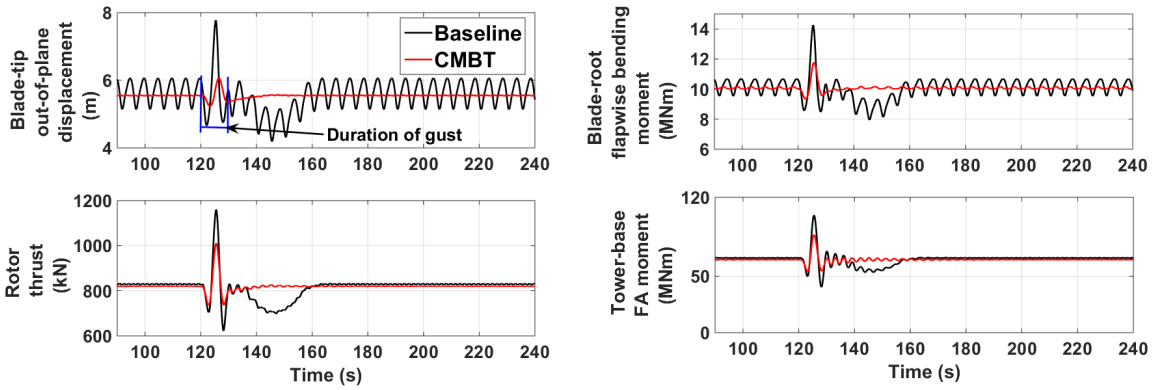

Figure 16. Turbine response to extreme operational gust (at rated wind speed).

in peak-to-peak response of over 50% for both load components.

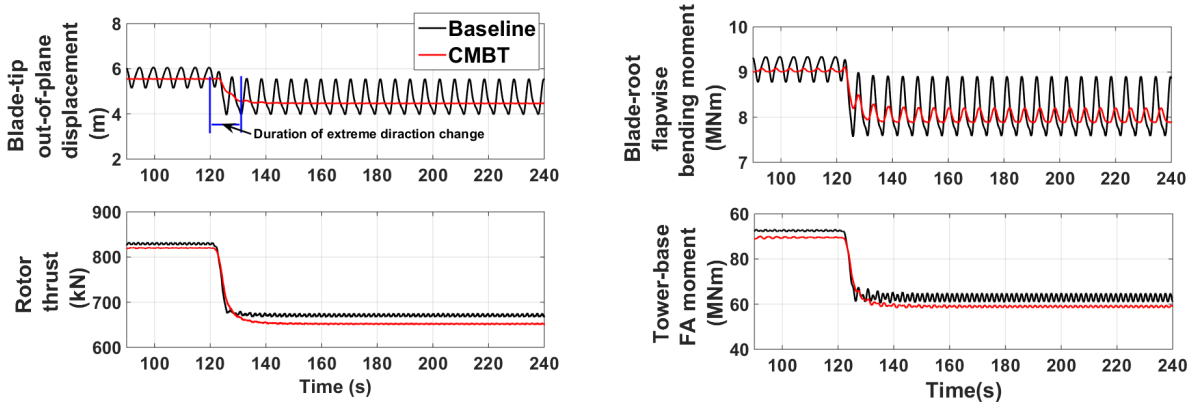

Figure 17. Turbine response to extreme direction change (at rated wind speed).

Overall, the controller is also able to reduce peak loads caused by extreme gust and extreme direction change. Furthermore, it should be noted that the critical load case for determining the ultimate loads is extreme turbulence during power production (DLC 1.3), since the magnitude of the peak responses from extreme turbulence exceed those from gust excitation or direction change.

VIII. Conclusions

An active control concept based on camber morphing blade tip (CMBT) is proposed for load mitigation on multi megawatt scale HAWTs. A span-wise variation of camber at the outer blade region is proposed that blends seamlessly to the non-morphing part of the rotor blade. The NREL 5MW reference turbine is used as baseline design, where the outer 30% of the blade is linearly cambered with the maximum camber realized at the blade tip. 30% of NACA60-618 airfoil's trailing edge is cambered on the basis of sufficient change in lift (Δc_l) without significant increase in drag (high $\frac{\Delta c_l}{\Delta c_d}$) compared to the baseline airfoil. A PID controller is implemented for the camber morphing blade tip. Several simulations in accordance with the IEC standard are carried out using the open source code FAST, after extending the capability of the software to include the effect of actively morphing the rotor blade during simulation.

The results show that the proposed method is capable of reducing vibratory and ultimate loads:

- The CMBT controller is able to reduce the fatigue loads for most of the wind turbine components. A reduction of 24% in fatigue load is observed for the flap-wise blade root bending moment when the CMBT controller is used. Furthermore, higher reduction in fatigue loads is observed for the pitch

and yaw moment at the tower-top, where the reduction is of the order 36%. However, the controller slightly increased the fatigue load for the edge-wise blade root moment. This could be the result of the controller design witch uses feedback of only out-of-plane blade tip measurements and no in-plane measurements. A control design based on the full dynamic state of the blade could result further reduction in fatigue loads for all wind turbine components.

- The controller is also able to mitigate the effect of extreme turbulence on various turbine components. Most notable reduction in extreme loads is for: out-of-plane blade tip displacement (31%), yaw moment at tower-top (61%), pitch moment at tower-top (51%), and fore-aft moment at the tower base (33%). The large reduction in ultimate loads indicate that the controller is able to reduce load imbalance across the rotor disk.

- Similar to the ultimate loads due to extreme turbulence, the controller is also able to minimize the peak-to-peak response of multiple turbine components due to various gust excitations given in the IEC standard. The reduction in turbine response due to extreme gust is 43% for the fore-aft moment at the tower base and 76% for the out-of-plane blade tip displacement. Furthermore, the controller is also able to mitigate the peak-to-peak response of the turbine due to extreme direction change, resulting in over 90% reduction of peak-to-peak response for the out-of-plane blade tip displacement.

- The highest contribution to the actuator activity for the CMBT controller, under periodic and stochastic (normal turbulence) excitation, is around $1P$ and $2P$. This is the consequence of the controller design, in that the controller is tuned to reduce the harmonic response of the out-of-plane blade tip displacement caused by periodic excitation. Furthermore, the average actuator activity is nearly constant across the wind speeds when used to mitigate fatigue loads.

Overall, the controller is able to mitigate both fatigue loads and ultimate loads due to extreme turbulence and different gust excitations. It should be noted that the present study does not consider the complete benefit of the load alleviating capability of CMBT actuator. The reduction in fatigue and ultimate loads means that wind turbine blades outfitted with CMBT controller can be designed lighter or longer for higher energy extraction without increase in weight. This will result in either increase of annual energy capture or reduced component cost, which will lower the cost of energy.

Acknowledgment

This study was funded by the New York State Energy Research and Development Authority (NYSERDA) under Award No. 58059, Continuously Conformable Wind-Turbine Blade Tip, with Mr. Gregory Pedrick as the Program Manager.

References

[1]Bottasso, C. L., Croce, A., Gualdoni, F., Montinari, P., and Riboldi, C. E., "Articulated blade tip devices for load alleviation on wind turbines," *Wind Energy Science*, Vol. 1, No. 2, 2016, pp. 297.

[2]Bottasso, C., Campagnolo, F., Croce, A., and Tibaldi, C., "Optimization-based study of bend–twist coupled rotor blades for passive and integrated passive/active load alleviation," *Wind Energy*, Vol. 16, No. 8, 2013, pp. 1149–1166.

[3]Bottasso, C. L., Croce, A., Gualdoni, F., and Montinari, P., "Load mitigation for wind turbines by a passive aeroelastic device," *Journal of Wind Engineering and Industrial Aerodynamics*, Vol. 148, 2016, pp. 57–69.

[4]Andersen, P. B., Henriksen, L., Gaunaa, M., Bak, C., and Buhl, T., "Deformable trailing edge flaps for modern megawatt wind turbine controllers using strain gauge sensors," *Wind Energy*, Vol. 13, No. 2-3, 2010, pp. 193–206.

[5]Bernhammer, L. O., van Kuik, G. A., and De Breuker, R., "Fatigue and extreme load reduction of wind turbine components using smart rotors," *Journal of Wind Engineering and Industrial Aerodynamics*, Vol. 154, 2016, pp. 84–95.

[6]Bergami, L. and Poulsen, N. K., "A smart rotor configuration with linear quadratic control of adaptive trailing edge flaps for active load alleviation," *Wind Energy*, Vol. 18, No. 4, 2015, pp. 625–641.

[7]Chow, R. and van Dam, C., "Computational investigations of deploying load control microtabs on a wind turbine airfoil," *45th AIAA Aerospace Sciences Meeting and Exhibit*, 2007, p. 1018.

[8]Baker, J., Standish, K., and van Dam, C., "Two-dimensional wind tunnel and computational investigation of a microtab modified S809 airfoil," *43rd AIAA Aerospace Sciences Meeting and Exhibit*, 2005, p. 1186.

[9]Nakafuji, D., van Dam, C., Michel, J., and Morrison, P., "Load control for wind turbines a non-traditional microtab approach, AIAA 2002-0054," *Proceedings of the 40th AIAA/ASME, Reno, NV, USA*, 2002.

[10]Yen, D., van Dam, C., Smith, R., and Collins, S., "Active load control for wind turbine blades using MEM translational tabs," *20th 2001 ASME Wind Energy Symposium*, 2001, p. 31.

[11]Jonkman, J. M. and Buhl Jr, M. L., "FAST User's Guide-Updated August 2005," Tech. rep., National Renewable Energy Laboratory (NREL), Golden, CO., 2005.

[12]Jonkman, J., Butterfield, S., Musial, W., and Scott, G., "Definition of a 5-MW reference wind turbine for offshore system development," *National Renewable Energy Laboratory, Golden, CO, Technical Report No. NREL/TP-500-38060*, 2009.

[13]Van Rooij, R., "Modification of the boundary layer calculation in RFOIL for improved airfoil stall prediction," *Report IW-96087R TU-Delft, the Netherlands*, 1996.

[14]Moriarty, P. J. and Hansen, A. C., "AeroDyn theory manual," Tech. rep., National Renewable Energy Lab., Golden, CO (US), 2005.

[15]Jonkman, B. J. and Buhl Jr, M. L., "TurbSim users guide," *National Renewable Energy Laboratory*, 2009.

[16]Buhl Jr, M. L., "RunIEC Users Guide," Tech. rep., National Renewable Energy Lab., USA., 2001.

[17]Bossanyi, E., Witcher, D., and Mercer, T., "Project UpWind: Controller for 5MW reference turbine," *Contract*, 2009, pp. 1–18.

[18]Commission, I. E. et al., "IEC 61400-1: Wind turbines part 1: Design requirements," *International Electrotechnical Commission*, 2005.

[19]Kalverla, P. C., Steeneveld, G.-J., Ronda, R. J., and Holtslag, A. A., "An observational climatology of anomalous wind events at offshore meteomast IJmuiden (North Sea)," *Journal of Wind Engineering and Industrial Aerodynamics*, Vol. 165, 2017, pp. 86–99.

[20]Hayman, G., "Mlife theory manual for version 1.00," *National Renewable Energy Laboratory, Golden, CO*, 2012.

[21]Hopman, P., Kunst, P., and Pronk, A., "A renewed interpretation method for fatigue measurements, verification of miners rule," *4th Eurobitume Symposium in Madrid*, Vol. 1, 1989, pp. 557–561.

[22]Barlas, A. K., *Active aerodynamic load control on wind turbines: Aeroservoelastic modeling and wind tunnel experiments*, 2011.

[23]Andersen, P. B., Gaunaa, M., Bak, C., Buhl, T., and Poulsen, N. K., *Advanced load alleviation for wind turbines using adaptive trailing edge flaps: sensoring and control*, Technical University of DenmarkDanmarks Tekniske Universitet, Department of Solid MechanicsInstitut for Faststofmekanik, 2010.